# Long-Ranged Attractive Forces between Neutral Surfaces Due to Amphiphile Aggregation

**Jan Forsman,*,† Bo Jönsson,‡ and Torbjörn Åkesson§**

*Physical Chemistry 2, Chemical Center, P.O. Box 124, S-221 00 Lund, Sweden*

*Received: October 29, 1997; In Final Form: April 16, 1998*

The interaction of two charged surfaces, neutralized by adsorption or deposition of charged amphiphilic molecules, has been investigated using Metropolis Monte Carlo simulations. Each surface can be considered as a two-dimensional electrolyte (plasma), and it is well-known that there is a weak attractive surface-surface interaction decaying as $h^{-3}$ ($h$ being the separation) in the absence of any salt between the walls. If a small fraction of the amphiphiles self-assemble and form highly charged aggregates, the attractive interaction increases significantly. The magnitude is much larger than the ordinary van der Waals attraction and the force can be substantial out to several thousand angstroms and is of course salt-dependent. That this can be a plausible mechanism for the very long-ranged forces sometimes observed between mica surfaces made hydrophobic by adsorption or deposition of charged amphiphiles.

## 1. Introduction

Two hydrophobic surfaces immersed in aqueous solution will attract each other. This is obvious, since bringing them into contact and thereby reducing the hydrophobic surface exposed to water will decrease the free energy. The range of this so-called hydrophobic attraction, however, has proven difficult to estimate. Despite a large number of experiments,[1−17] there is little firm knowledge about it. Not only does the measured range of the force differ by an order of magnitude between experiments but the reports of, for instance, the salt dependence are even in qualitative disagreement.[3,8,9,10,15,17] A number of theoretical attempts have been made to provide plausible molecular mechanisms explaining the experimental results. These include hydrogen bond propagation,[18] long-ranged correlations near the spinodal point,[19,20] various kinds of cavity/bubble formation,[15−21] hydrodynamic fluctuations,[26] and depressed density of the confined solvent.[27] It has also been suggested that correlations between charged domains on the surfaces[12,28−32] can give rise to a long-ranged attraction. This last mechanism has, in our opinion, not been satisfactorily investigated, and in this paper we will use Monte Carlo (MC) simulations to study the interaction between two net neutral surfaces with highly charged aggregates. These domains or inhomogeneities may or may not be present when the surfaces are isolated, but, as we shall see, they may be too small to be detected and yet dominate the attraction even at large distances. If the heterogeneities are present when the surfaces are isolated, the reason for them to appear is probably a reduction of interfacial tension. One could also speculate that the mean amphiphile density at the surfaces lies in a two-dimensional "gas−liquid" coexistence region. If so, the thermodynamically most stable state would probably be attained by a division of the surface into liquid and gas regions of macroscopic dimensions. However, once a few microscopic liquid islands, or "blobs", have formed, the electrostatic repulsion between them may provide a stabilizing free energy barrier that prevents further coagulation. These high-density regions may of course also be large enough to be detected experimentally, and Manne et al.[33] have indeed observed amphiphilic aggregates of various shapes on such surfaces.

The present study will be restricted to net neutral surfaces, but one should note that adsorption/desorption with a possibility of transport of amphiphiles from one surface to the other could further increase the attraction.[34−36] We will also fix the size of the aggregates formed on the surfaces, but one should note that if their existence is due to intersurface interactions, their size and number may increase as the separation gets smaller, which would enhance the attraction further. Before describing our calculations, we shall briefly discuss the hydrophobic force and its range in more general terms.

## 2. Neutral Surfaces and Attractive Forces

Most experimental studies of the hydrophobic force have been performed with the so-called surface force apparatus.[37] Here the surfaces usually consist of mica glued onto crossed cylinders. In aqueous solution the mica will ionize and aquire a net negative charge, of the order $-0.3$ C/m$^2$. These hydrophilic mica surfaces can be made hydrophobic in a number of ways. The most relevant methods that lead to systems represented by our model (for which comparisons with our theoretical data is possible) are where a cationic surfactant is deposited onto mica with the Langmuir−Blodgett technique or where the mica surfaces adsorb surfactant molecules from solution. In both these experimental situations, one finds long-ranged attractive forces.[4,5,8−10,12] The mica surfaces can also be made hydrophobic by a covalently bound layer. Thus, one can distinguish at least two clearly different experimental situations. We believe that the attractive forces seen in these two cases are of completely different origin.

It is often claimed that the range of the measured force, 100−1000 Å, is surprisingly large but one could in fact argue that it "should" be much larger. The solvent contribution to the interaction free energy per unit area, $G_s(h)$, for two macroscopically large flat surfaces separated a distance $h$ may be written:[38]

$$G_s(h) = (P_b - P_{||}(h))h \tag{1}$$

where $P_b$ is the external bulk pressure and $P_{||}(h)$ is the (uniquely defined) average component of the pressure tensor acting parallel

† E-mail address: jan.forsman@fkem2.lth.se.
‡ E-mail address: bo.jonsson@fkem2.lth.se.
§ E-mail address: torbjorn.akesson@fkem2.lth.se.

S1089-5647(98)00022-4 CCC: $15.00 
Published on Web 06/06/1998

to the surfaces. The average is taken across the slit formed by the surfaces, i.e.,

$$P_{\parallel}(h) = \frac{1}{h}\int_0^h \mathrm{d}z\, P_t(z) \tag{2}$$

where $P_t(z)$ is the local (not uniquely defined) parallel component of the pressure tensor at a distance $z$ from one of these surfaces. At large separations, $G_s$ approaches twice the value of the bulk interfacial tension at a single surface. As long as $P_{\parallel}(h)$ is positive, there may exist a stable liquid phase between the surfaces. However, as the surfaces approach, $P_{\parallel}$ is reduced and will eventually become zero at some separation $h_s$, where a thermodynamically stable liquid phase no longer exists. By using typical values for the bulk pressure (1 bar) and water−hydrocarbon interfacial tension (50 mJ/m$^2$), we can estimate $h_s$ to be about 1 $\mu$m! In obtaining this number, we have neglected the $h$-dependence of $G_s$ and simply set it equal to its bulk value, at infinite separation. That this is a good approximation at such large separations is confirmed by the absence of a detectable force.

Recently, an attempt to simulate the pure solvation force was made,[39] and the simulations, which had to be restricted to short separations and high bulk pressures, indicated that the confined liquid water should become unstable below 10 Å. Interestingly, if we again neglect the separation dependence in the interaction free energy and use the estimated bulk pressure (1500 bar) and surface tension (80 mJ/m$^2$) provided by the simulations in ref 39, we obtain $h_s = 11$ Å, which is surprisingly close to the value found in the simulations. This agreement is of course to some extent fortuitous, but it suggests that at atmospheric pressure it is indeed surprising that liquid water confined between hydrophobic surfaces does not evaporate at distances much larger than those where most experiments are performed. Apparently, the nucleation free energy barrier is high and provides a kinetic stabilization. However, there is the additional possibility that the surfaces change, either by structural rearrangement or by desorption/adsorption, as they are brought closer together. This could lower the interfacial tension and stabilize the confined liquid. Obviously, such a change of the surfaces must involve a free energy cost, which has to be more than compensated by an increased attractive interaction with the other surface. If such a correlation is to be important even at large separations, one would expect it to originate from a charge−charge interaction.

A negatively charged surface, rendered neutral by adsorption of amphiphiles, forms a two-dimensional electrolyte, and a pair of such surfaces will attract each other in solution. This situation has been studied theoretically by several groups over the years.[28,30,32,40] If the confined liquid (water) contains no added salt, a particularly simple case appears, for which one can show that the pressure decays asymptotically as

$$P_{As} = -\frac{k_B T \zeta(3)}{8\pi h^3} \tag{3}$$

where $k_B$ is Boltzmann's constant and $\zeta(3)$ is a Riemann $\zeta$ function and approximately equal to 1.2. An interesting feature of eq 3 is its universality, since it does not depend on details of the charges on the surface. This means that the asymptotic force will be the same whether the amphiphiles form large aggregates or exist in monomeric form, but the equation says nothing of where the asymptotic regime is reached. Adding salt will screen the interactions, giving rise to a number of different cases, i.e., different types of surfaces, which have been investigated within the Debye−Hückel approximation.[41] The interaction between surfaces carrying mobile charges is described by the so-called Ninham−Parsegian expression for the pressure, which has the following limiting forms

$$P \sim -\frac{k_B T}{(\kappa h)^3} \qquad h \ll \kappa^{-1} \tag{4}$$

$$P \sim -k_B T \kappa^3 \frac{\mathrm{e}^{-2\kappa h}}{\kappa h} \qquad h \gg \kappa^{-1} \tag{5}$$

with $\kappa$ denoting the Debye screening length. The attraction in the "preasymptotic" regime is expected to be stronger if the amphiphiles condense to form blobs with a high charge on the surfaces than if they appear as monomers. Several theoretical attempts have been made to estimate the short separation behavior of the force analytically,[12,29,31] but in these approaches a periodic structure on the surfaces as well as the validity of the linearized Poisson−Boltzmann approximation is assumed. To avoid such restrictions, one has to abandon the analytical approach and resort to simulation methods.

## 3. Model Description

The underlying physical model we used was a negatively charged surface with a surface charge density equal to −0.32 C/m$^2$, corresponding to −50 Å$^2$/$e$, $e$ being the elementary charge. The surfaces were rendered neutral by deposition of cationic amphiphiles. However, the amphiphiles were assumed to be heterogeneously distributed, forming circular blobs with a total charge $Q$ and radius $R$ as well as existing in monomeric form. The monomeric amphiphiles were not explicitly included in the simulations, but assumed to partly neutralize the mica surfaces leading to a decreased surface charge density. The surface charge density in the aggregates was taken to be 0.40 C/m$^2$, slightly larger in magnitude than the bare mica value. Thus, the simulated system consisted of positively charged blobs moving on two parallel and uniformly charged surfaces separated by a dielectric continuum. No image charge effects were considered, i.e., the dielectric was assumed to extend beyond the surfaces. Asymtotically, the surface force in this system will approach the net force, including the van der Waals interaction, acting between two surfaces at which there are dielectric discontinuities.[28]

Salt was added in some of the simulations and salt ions were free to move in the volume delimited by the surfaces—see Figure 1 for a schematic description. The blobs were not allowed to approach each other closer than 2$R$ in the simulations, but this restriction turned out to be superfluous since the repulsion between them was sufficient to prevent such encounters. In the presence of salt the number of particles (ion pairs) was chosen so as to maintain equilibrium with a bulk salt solution, i.e., to keep the sum of their individual chemical potentials constant. Only monovalent ions were used, and they were modeled as hard spheres, with a radius of 2 Å, and were not allowed to approch the surfaces closer than one hard sphere diameter. The bulk chemical potential was calculated using the Debye−Hückel theory, which is a reliable approximation at the low salt concentrations considered here (<0.1 mM). Interactions between blobs were evaluated by interpolation between neighboring elements in a vector containing numerically calculated energies and forces. Interactions between a blob and an ion was evaluated in a similar manner, but this time a matrix had to be used. The simulations were performed using the traditional Metropolis Monte Carlo algorithm, with periodic boundary

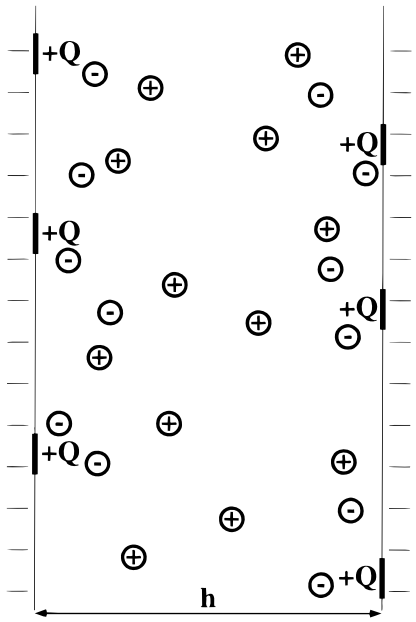


**Figure 1.** Schematic picture of the system under study.

conditions in the lateral directions (parallel with the surfaces), and the minimum image convention was used to truncate the potentials. The temperature was 300 K and water was modeled as a dielectric continuum, with dielectric constant $\epsilon_r = 78$. We denote by $L$ the lateral length of the simulation box, whereas $h$ is the separation between the two surfaces. Further, we let $z$ be the direction normal to the walls and put $z = 0$ at the left wall. The number of blobs on one surface in the simulation cell is $N$, and the underlying "background" charge density, due to the monomeric amphphiles and the mica surface, is given by $\sigma = -NQ/L^2$. The lateral extent of the simulation box was in all simulations more than 10 times as large as the separation between the surfaces. Size dependence checks were performed, and such effects were found to be negligible. Since the density profiles of the ions in the slit were rapidly varying, technical efforts were made to improve the statistics of simulations including salt. Some Monte Carlo moves consisted of a mirror reflection across the midplane, followed by an attempted random insertion at the new $z$-coordinate. Also, the displacement parameter for $x,y$-translations of ions was usually twice as large as in the $z$-direction. Occasionally (with a prescribed frequency) a much larger displacement parameter was used in the $x,y$-directions.

The chemical potential was evaluated in a central slab $\Omega$ of the slit, excluding regions located within 50 Å from each surface. The excess contribution to the chemical potential was calculated using Widom's[42] method, and owing to the low salt concentration a net neutral salt pair could be used at each insertion. If the mean density of ion $\alpha$ within region $\Omega$ is $\langle c_\alpha \rangle_\Omega$, the chemical potential $\mu_\alpha$ of this ion may be written

$$\beta\mu_\alpha = \ln \langle c_\alpha \rangle_\Omega - \ln \langle \exp(-\beta \Delta U_\alpha) \rangle_\Omega \tag{6}$$

where $\Delta U_\alpha$ is the interaction between a test particle of species $\alpha$, inserted in region $\Omega$, with the rest of the system, including the other test ion of opposite charge. The kinetic part of the chemical potential is of course unchanged between bulk and slit, so we exclude it from our treatment. Given a value of the chemical potential in the slit from simulations, the corresponding bulk salt concentration was calculated using Debye−Hückel theory, according to which

$$\mu = 2k_B T \ln c_s(\text{bulk}) - \frac{\kappa e^2}{4\pi\epsilon_0\epsilon_r} \tag{7}$$

with $c_s$ being the salt concentration in the bulk and $\mu$ the chemical potential of a salt pair. As usual, the permittivity of vacuum is denoted by $\epsilon_0$. In the simulations, repeated runs were performed until the chemical potential found was within 0.01 $k_B T$ (about one standard deviation) from the prescribed bulk value. Let $\Gamma$ and $Y$ denote the regions $z < h/2$ and $z > h/2$, respectively. If we define the potential $\Phi(z)$

$$\Phi(z) = \frac{2z}{4\pi\epsilon_0\epsilon_r}\left[\arcsin\left(\frac{a^4 - z^4 - 2a^2z^2}{(a^2+z^2)^2}\right) + \frac{\pi}{2}\right] - \frac{8a}{4\pi\epsilon_0\epsilon_r}\ln\left[\frac{\sqrt{2a^2+z^2}+a}{\sqrt{a^2+z^2}}\right] \tag{8}$$

where $a = L/2$, the interaction energy between a blob of charge $Q$ and the smeared-out background charge on the opposite surface is given by $Q\sigma\Phi(h)$, providing a force $-Q\sigma\partial\Phi(h)/\partial h$ on the walls. Thus, the pressure, $P_0$, on the walls is in the absence of salt given by

$$P_0 = \frac{1}{L^2}\left[\sum_{j\in\Gamma}^{N}\sum_{k\in Y}^{N} F_{jk}^{bb} - N\sigma\frac{\partial\Phi(h)}{\partial h}\right] \tag{9}$$

where $F_{jk}^{bb}$ is the $z$-component of the force acting between blobs $j$ and $k$. With salt present, one also has to include pressure contributions arising from ion−ion, ion−blob, and ion−background surface charge interactions across the midplane. Furthermore, there is an ideal contribution arising from the difference between the total salt concentration at the midplane and the bulk salt concentration.[43] Since the concentrations of salt we consider are very low (<0.1 mM), contributions to the pressure from collision terms at the midplane were entirely negligible. Thus, we may write the net pressure, $P_{net}$, in the presence of salt as

$$P_{net} = P_0 + k_B T\left(c_+\left(\frac{h}{2}\right) + c_-\left(\frac{h}{2}\right) - 2c_s(\text{bulk}) - \frac{\kappa^3}{24\pi}\right) + \frac{1}{L^2}\left[\sum_{n\in\Gamma}\sum_{j\in Y}^{N} F_{nj}^{ib} + \sum_{m\in Y}\sum_{k\in\Gamma}^{N} F_{mk}^{ib} + \sum_{n\in\Gamma}\sum_{m\in Y}\frac{|z_n - z_m| q_n q_m}{4\pi\epsilon_0\epsilon_r|\mathbf{r}_n - \mathbf{r}_m|^3}\right] - \frac{\sigma}{L^2}\left[\sum_{n\in\Gamma} q_n\frac{\partial\Phi(h-z_n)}{\partial(h-z_n)} + \sum_{m\in Y} q_m\frac{\partial\Phi(z_m)}{\partial(z_m)}\right] \tag{10}$$

where summation indices $m$ and $n$ denotes ions while $i$ and $j$ are used for the blobs. $F_{\alpha\gamma}^{ib}$ denotes the $z$-projection of the force between ion $\alpha$ and blob $\gamma$, and $c_+(h/2)$ and $c_+(h/2)$ denote the midplane concentrations of positive and negative ions, respectively. Finally, $q_\alpha$ and $\mathbf{r}_\alpha$ are the charge and coordinate of ion $\alpha$.

## 4. Results

Specifications of system parameters and notations used in this work are provided in Table 1 and in Figure 1. In Figure 2, the pressure curves for the systems described in Table 1 are shown and compared with a typical van der Waals interaction, decaying as $-A_H/h^3$, as well as the asymptotic expression, $P_{As}$. Note that even a very small surface inhomogeneity is sufficient to cause an attraction that by far exceeds the expected van der

**TABLE 1: System Parameters**[a]

| system | $-\sigma$/(mC/m$^2$) | $Q/e$ | $R$/Å | $c_s$/mM |
|---|---|---|---|---|
| A0 | 1.92 | 30 | 44 | 0 |
| A1 | 1.92 | 30 | 44 | 0.46 |
| A2 | 1.92 | 30 | 44 | 0.92 |
| B0 | 3.84 | 30 | 43 | 0 |
| B1 | 3.84 | 30 | 43 | 0.46 |

[a] $\sigma$ is the surface charge density on the partly neutralized mica surface, and $Q$ and $R$ are the blob charge and radius, respectively.

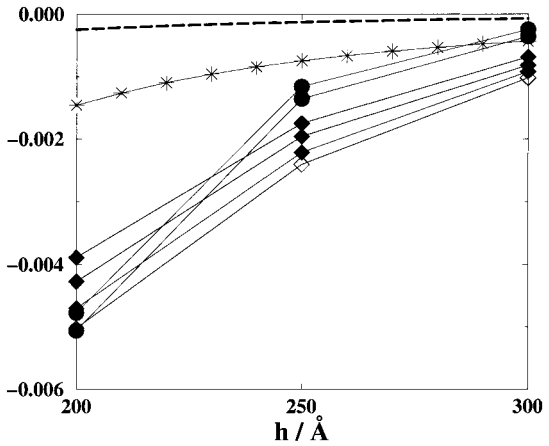


**Figure 2.** Simulated pressures for the systems described in Table 1. Filled diamonds: A0−A2, in order of decreasing attraction. As an indication of blob size effects, results with R = 0, but otherwise identical parameters as A0, are given by open diamonds. Cirles: B0 and B1, in order of decreasing attraction. Stars: the van der Waals attraction, with a Hamaker constant of $A_H = 2.2 \times 10^{-20}$ J. Dashed line: the universal asymptotic expression for the correlation attraction. The two latter curves differ by approximately a factor of 6.

Waals interaction. The extra attraction pertains to large separations, and the asymptotic limit is only reached at very large separations. In the systems studied in Figure 2 more than 95% of the mica charge is neutralized by free monomeric amphiphiles and less than 5% is covered by a blob. Note that for salt-free systems, our use of circular blobs of finite size instead of point charges has no profound importance. However, when there is salt present, the blob construction is essential, since a localized point charge on the blobs would give rise to unrealistic salt distributions.

We also see in Figure 2 that the presence of salt has a significant effect, even at very small concentrations. Thus, if correlations between regions of high amphiphile density are important in measurements of the force between hydrophobic surfaces, the observed force will be affected by addition of salt. In the parameter range we have examined in this study, the attraction decreases with increasing salt concentration. Note, however, that the effect an increased salt concentration has on the surface structure and the force between the surfaces is complicated by the fact that the nearest-neighbor separation between blobs is similar to the surface−surface separation. Adding salt will of course screen blob−blob correlations across to the other surface. On the other hand, the intrasurface screening may facilitate a stronger intersurface correlation. In other words, it is quite possible that for some other parameter choices, one would find that addition of salt increases the attraction. The correlations are visualized in the blob−blob radial distribution functions, given in parts a and b of Figure 3, for $h = 200$ and 300 Å, respectively. We see that even the qualitative change in the correlations caused by salt screening varies with separation. That is, adding salt at a separation of 200 Å reduces the intersurface correlations, while it slightly

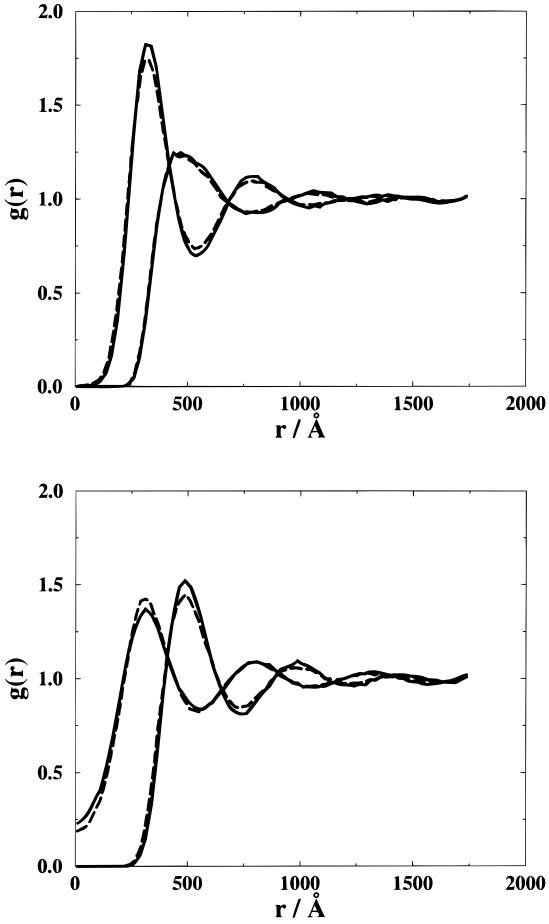


**Figure 3.** Blob−blob radial distribution functions, for systems A0 (solid) and A2 (dashed). The "radius", $r$, is in this case the projected distance $(x^2 + y^2)^{1/2}$, where $x$ and $y$ are orthogonal directions parallel with surfaces. The distribution functions between blobs at the same surface are those that are zero out to a distance of about 250 Å. (a, top) $h = 200$ Å. (b, bottom) $h = 300$ Å.

increases the intrasurface correlations. The opposite is true at 300 Å. Thus, we clearly see how the two length scales, the blob−blob separation and the surface-to-surface separation, affect the system. If the latter is much larger than the former, the asymptotic law, eq 3, probably provides a good description of the interaction, while in the other extreme one can expect large deviations from the asymptote. Experimentally, there seem to be no consensus on the salt dependence of the measured force. If the blobs are highly charged and the concentration of blobs is increased sufficiently, a freezing transition will take place. This will for instance occur in our simulations for surfaces with blob charge $Q = 60\ e$ and $\sigma = -1.92$ mC/m$^2$. The freezing transition will be separation-dependent, and it is therefore possible that an initially amorphous surface structure will freeze as the separation is reduced, which most likely would increase the attraction in a stepwise manner. However, there is also a possibility of the reverse process, that the blobs crystallizes on the surfaces as the separation becomes sufficiently large.

We now proceed to a more systematic study of how the range and magnitude of the correlation attraction depend on the blob charge and blob density, in the absence of salt. For simplicity we will use "point blobs", i.e., set $R = 0$. As we saw in Figure 2, this does not appreciably affect the results. If we keep $\sigma$ constant but increase the blob charge, we obtain a stronger and more long-ranged attraction, as shown in Figure 4, where we have normalized the pressure by the universal asymptote, $P_{As}$. The maximum of this "reduced" pressure is shifted to a larger

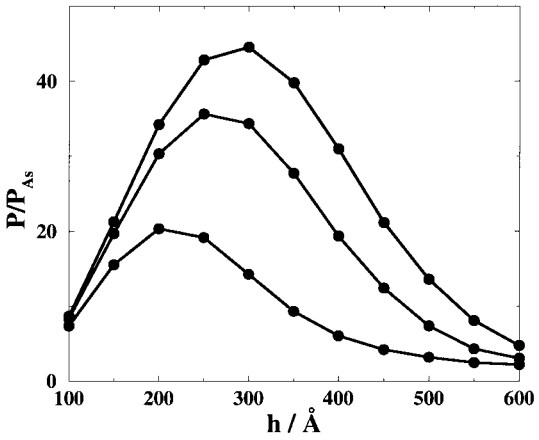


**Figure 4.** Attractive correlation pressure, reduced by the asymptotic limit, $P_{As}$, for surfaces, all with $\sigma = -1.92$ mC/m$^2$ but with different values of the blob charge, $Q$. For, simplicity "point blobs", with $R = 0$, were used. From bottom to top: $Q = 30$, 42, and 48 $e$.

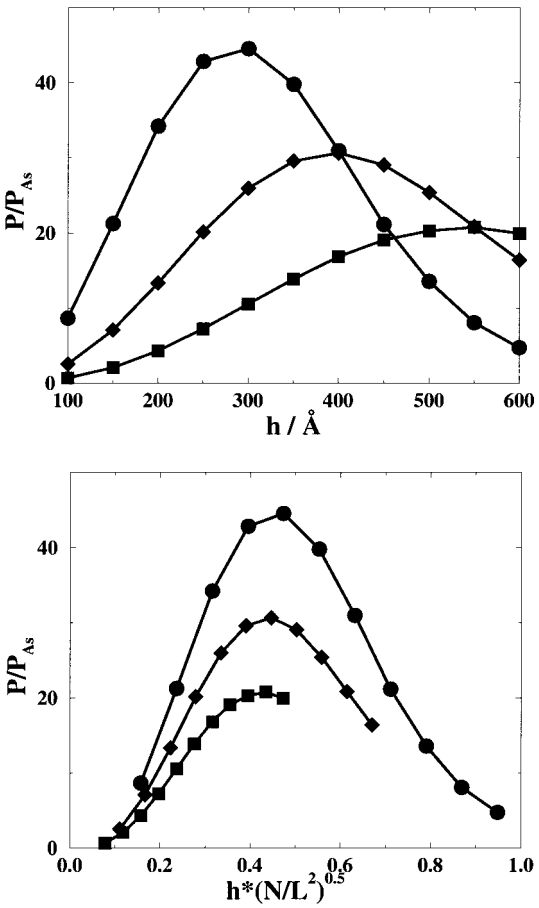


**Figure 5.** (a, top) Attractive correlation pressure, reduced by the asymptotic limit, $P_{As}$, for surfaces with blobs of fixed charge $Q = 48$ $e$ but with different blob densities. Circles, diamonds, and squares are for $\sigma = -1.92$, $-0.96$, and $-0.48$ mC/m$^2$, respectively. (b, bottom) Same as in (a), but with the separation being normalized by the square root of the blob density.

separation as the blob charge is increased; i.e., the attraction then becomes more long-ranged. The reason is that the asymptotic limit is not approached unless the surface separation is larger than a typical nearest-neighbor separation between blobs at the same surface. The separation at which the reduced pressure show a maximum, $h_{max}$, scales approximately inversely with the square root of the blob surface density, which can be considered as a characteristic length in the system. In Figure

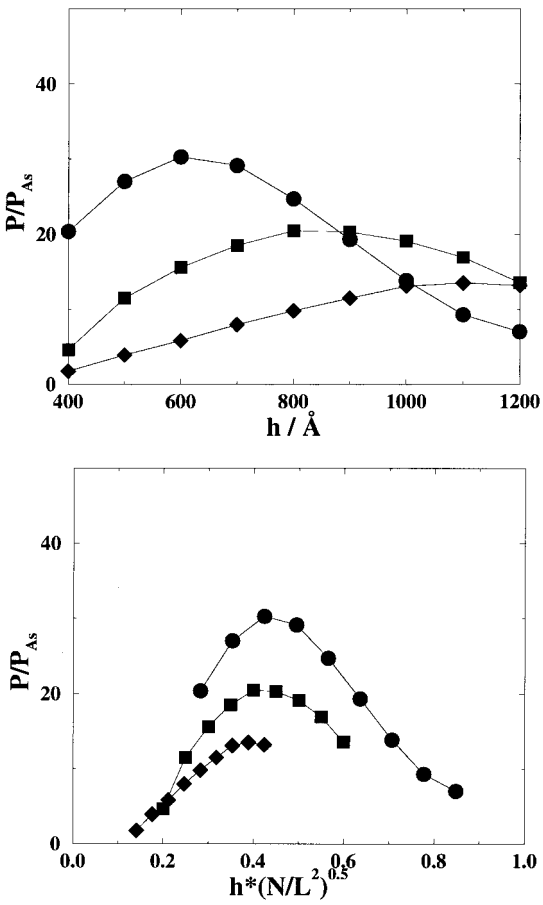


**Figure 6.** (a, top) Attractive correlation pressure, reduced by the asymptotic limit, $P_{As}$, for surfaces with blobs of fixed charge $Q = 60$ $e$ but with different blob densities. Circles, diamonds, and squares are for $\sigma = -0.48$, $-0.24$, and $-0.12$ mC/m$^2$, respectively. (b, bottom) Same as in (a), but with the separation being normalized by the square root of the blob density.

4, we can also observe how the maximum of the reduced pressure increases with blob charge, the reason being a stronger intersurface coupling. In Figure 5a, the reduced pressure varies with the blob surface density, for a fixed blob charge, $Q = 48e$. Again we can see how the "extra" attraction becomes more long-ranged as the blob density is decreased but also how the reduced pressure maximum is shifted downward. To show more clearly that $h_{max}$ scales inversely with the square root of the blob surface density, we have performed such a scaling of the separation in Figure 5b. Finally, in Figure 6 we exemplify how, with high blob charges and low surfaces densities, one can obtain an extremely long ranged attraction, of the order 1000 Å.

## 5. Conclusions

It seems likely that the correlation attraction studied in this work is important in some of the experiments, where hydrophobic surfaces are formed by adsorption of charged amphiphiles from solution or by deposition using the Langmuir−Blodgett technique. Our results suggest that the major qualitative conclusions drawn in the recent studies by Tsao et al.[12] and Miklavic et al.[31] are essentially correct, albeit the theoretical treatments included a number of simplifying assumptions. It would be improper to use the term hydrophobic attraction for the type of force investigated here, as it has very little to do with hydrophobic interactions involved in, for instance, protein folding or micelle formation. It is probably not related to the attractive interaction seen between covalently hydrophobized

mica surfaces either. In these systems there presumably exist important interactions more directly related to the solvent properties. Pure solvent effects such as solvent metastability and/or density depression[27] may be important in such systems, as opposed to direct surface interactions of the kind examined here. A further conclusion is that even small deviations from a "perfectly" organized experimental setup can give rise to forces of a different nature from the ones supposedly under study. Hopefully this will lead to a more cautious interpretation of experimental results found using, for instance, the surface force apparatus or the atomic force microscope. A search for experimental methods with which the hydrophobic interaction can be directly studied in the physical systems where they are expected to be important is certainly called for. An interesting example of such a direct method has recently been described by van de Ven et al.,[44] measuring forces between latex spheres of colloidal dimensions, although so far only charged particles have been studied. Considering the drawbacks of the present measuring techniques, there is at present no evidence that water will induce a significant attraction of non van der Waals origin at large distances between hydrophobic particles.

**Acknowledgment.** We thank Stan Miklavic and Rudi Podgornik for comments and criticism.

## References and Notes

(1) Israelachvili, J. N.; Pashley, R. M. *J. Colloid Interface Sci.* **1984**, *98*, 500.
(2) Pashley, R. M.; McGuiggan, P. M.; Ninham, B. W.; Evans, D. F. *Science* **1985**, *229*, 1088.
(3) Claesson, P. M.; Blom, C. E.; Herder, P. C.; Ninham, B. W. *J. Colloid Interface Sci.* **1986**, *114*, 234.
(4) Claesson, P. M.; Christenson, H. K. *J. Phys. Chem.* **1988**, *92*, 1650.
(5) Christenson, H. K.; Claesson, P. M. *Science* **1988**, *239*, 390.
(6) Kekicheff, P.; Christenson, H. K.; Ninham, B. W. *Colloids Surf.* **1989**, *40*, 31.
(7) Kurihara, K.; Kato, S.; Kunitake, T. *Langmuir* **1992**, *8*, 557.
(8) Christenson, H. K.; Fang, J.; Ninham, B. W.; Parker, J. L. *J. Phys. Chem.* **1990**, *94*, 8004.
(9) Tsao, Y.-H.; Evans, D. F. *Langmuir* **1991**, *7*, 3154.
(10) Christenson, H. K.; Claesson, P. M.; Parker, J. L. *J. Phys. Chem.* **1992**, *96*, 6725.
(11) Parker, J. L.; Claesson, P. M. *Langmuir* **1992**, *8*, 757.
(12) Tsao, Y.-H.; Evans, D. F.; Wennerström, H. *Science* **1993**, *262*, 547.
(13) Parker, J. L.; Yaminsky, V. V.; Claesson, P. M. *J. Phys. Chem.* **1993**, *97*, 7706.
(14) Parker, J. L.; Claesson, P. M. *Langmuir* **1994**, *10*, 635.
(15) Parker, J. L.; Claesson, P. M.; Attard, P. *J. Phys. Chem.* **1994**, *98*, 8468.
(16) Kekicheff, P.; Spalla, O. *Phys. Rev. Lett.* **1995**, *9*, 1851.
(17) Wood, J.; Sharma, R. *Langmuir* **1995**, *11*, 4797.
(18) Eriksson, J. C.; Ljunggren, S.; Claesson, P. M. *J. Chem. Soc., Faraday Trans. 2* **1989**, *85*, 163.
(19) Attard, P.; Ursenbach, C. P.; Patey, G. N. *Phys. Rev. A* **1992**, *10*, 7621.
(20) Berard, D. R.; Attard, P.; Patey, G. N. *J. Chem. Phys.* **1993**, *98*, 7236.
(21) Yaminsky, V. V.; Yuschenko, V. S.; Amelia, E. A.; Schkukin, D. *J. Colloid Interface Sci.* **1983**, *96*, 301.
(22) Yuschenko, V. S.; Yaminsky, V. V.; Schkukin, D. *J. Colloid Interface Sci.* **1983**, *96*, 307.
(23) Craig, V. S.; Ninham, B. W.; Pashley, R. M. *J. Phys. Chem.* **1993**, *98*, 8468.
(24) Ducker, W. A.; Xu, Z.; Israelachvili, J. N. *Langmuir* **1994**, *10*, 3279.
(25) Eriksson, J. C.; Ljunggren, S. *Langmuir* **1995**, *11*, 2325.
(26) Ruckenstein, E.; Churaev, N. *J. Colloid Interface Sci.* **1991**, *147*, 535.
(27) Forsman, J.; Woodward, C. E.; Jönsson, B.; Wennerström, H. *J. Phys. Chem.* **1997**, *101*, 4253.
(28) Attard, P.; Kjellander, R.; Mitchell, D. J.; Jönsson, B. *J. Chem. Phys.* **1988**, *89*, 1664.
(29) Richmond, P. *J. Chem. Soc., Faraday Trans. 2* **1992**, *96*, 1066.
(30) Podgornik, R. *J. Chem. Phys.* **1989**, *91*, 5840.
(31) Miklavic, S. J.; Chan, D. Y. C.; White, L. R.; Healy, T. W. *J. Phys. Chem.* **1994**, *98*, 9022.
(32) Belloni, L.; Spalla, O. *J. Chem. Phys.* **1997**, *107*, 465.
(33) Manne, S.; Hermann, E. G. *Science* **1995**, *270*, 1480.
(34) Podgornik, R.; Parsegian, V. A. *Chem. Phys.* **1991**, *154*, 477.
(35) Podgornik, R.; Parsegian, V. A. *J. Phys. Chem.* **1995**, *99*, 9491.
(36) Ennis, J.; Sjöström, L.; Åkesson, T.; Jönsson, B. *J. Phys. Chem., in press*.
(37) Israelachvili, J. N.; Adams, G. E. *J. Chem. Soc., Faraday Trans. 1* **1978**, *74*, 975.
(38) Rowlinson, J. S.; Widom, B. *Molecular Theory of Capillarity*; Oxford University Press: Oxford, 1982.
(39) Forsman, J.; Jönsson, B.; Woodward, C. E. *J. Phys. Chem.* **1996**, *100*, 15005.
(40) Attard, P.; Kjellander, R.; Mitchell, D. J. *Chem. Phys. Lett.* **1987**, *139*, 219.
(41) Mahanty, J.; Ninham, B. W. *Dispersion Forces*; Academic Press: London, 1976.
(42) Widom, B. *J. Stat. Phys.* **1963**, *39*, 2808.
(43) Evans, D. F.; Wennerström, H. *The Colloidal Domain*; VCH Publishers: New York, 1994.
(44) van de Ven, T. G. M.; Warszynski, P.; Wu, X.; Dabros, T. *Langmuir* **1994**, *10*, 3046.